Preparation and Characterization of Electropolymerized Poly(*N*-Substituted Methacrylamide) Matrices on Graphite Fibers

JENG-LI LIANG,[1] JAMES P. BELL,[1,*] and DANIEL A. SCOLA[2]

[1]Institute of Materials Science, University of Connecticut, Storrs, Connecticut 06269-3136 and
[2]United Technologies Research Center, East Hartford, Connecticut 06108

SYNOPSIS

2- or 4-carboxyphenyl methacrylamide (2- or 4-CPM) was successfully electrocopolymerized with either methylmethacrylate (MMA) or *N*-phenylmaleimide (NPMI) to form a thick thermoplastic matrix with high glass-transition temperature (200–300°C), on Hercules AS-4 graphite fibers. The dependence of the diffusion of active species through the coating upon the solvent/water ratio in the cell was estimated from the electrochemical diffusion behavior of hexacyanoferrate(III) ions. A higher solvent/water ratio helped to increase polymer weight gain by increasing the solvent swelling and increasing the diffusion coefficient of active species. A highly solvent-swollen polymer layer promoted the rate of polymer weight gain. The copolymer composition of 4-CPM/MMA and 4-CPM/NPMI polymers was random, and the effects of variables were consistent with free-radical polymerization kinetics. The electropolymerization rates of 4-CPM/MMA and 4-CPM/NPMI were increased by increasing current density and monomer concentration. For a slight temperature increase (from 28–45°), electropolymerization rate and polymer weight gain increased dramatically for the 4-CPM/NPMI system. © 1993 John Wiley & Sons, Inc.

INTRODUCTION

Graphite fiber composites using thermoplastic polymer matrices have been the subject of a number of investigations[1-5] in recent years, mainly because of their improved fracture toughness and greater strain-to-failure relative to thermosets. Thermoplastics do not require a lengthy curing cycle and can be postformed by the application of heat and pressure. Due to low solubility and high viscosity of these thermoplastic matrices, fabrication of prepregs by melt impregnation or solution impregnation techniques is relatively costly and difficult.

The first application of aqueous electropolymerization to carbon fibers was investigated by Subramanian and Jakubowski.[6,7] Following their work, several recent publications[8-15] have shown that not only may a ductile interlayer be deposited onto graphite fibers but, under favorable conditions, the entire matrix may be electropolymerized onto the fibers. In this process, monomers are electropolymerized onto graphite fibers that have been wound around a rectangular frame and that function as the cathode in an electrochemical reaction cell. After the completion of polymerization, the polymer-coated graphite fiber plies are removed from the reaction cell, dried, and then become graphite fiber prepregs, suitable for composite fabrication by compression molding. This technique for fabrication of prepregs is rather simple and inexpensive, and could be adapted to a continuous process. Some other advantages are as follows:

(1) The weight gain (coating thickness) is easily controlled by the applied current and voltage.
(2) The composition of an interlayer or matrix can be controlled by proper choice of monomer, comonomer, and reaction conditions.
(3) Better adhesion can be obtained due to *in situ* polymerization at the fiber surface and

* To whom correspondence should be addressed.

Journal of Applied Polymer Science, Vol. 48, 477–494 (1993)
© 1993 John Wiley & Sons, Inc. CCC 0021-8995/93/030477-18

because the initial wetting of the fibers by monomer solution is favorable relative to wetting by a polymer.

Therefore, thermoplastic composites fabricated from electropolymerized monomers on graphite fibers may be the most promising alternative approach to overcome the fabrication problems of state-of-art thermoplastic composites.

MacCallum and MacKerron[16] have reported the growth of polyacrylamide films with 15% weight gain on graphite fibers by electropolymerization. Iroh, Bell, and Scola[13,14] have also reported the electropolymerization of both acrylamide and *N,N*-dimethylacrylamide onto graphite fibers with more than 200% weight gain. Unfortunately acrylamides as a class are easily swollen by water and have relatively low T_g. Therefore, one route to high T_g thermoplastic matrices is to incorporate bulky, stiff, and hydrophobic moieties onto at least part of the acrylamide monomer molecules. The present investigation deals with the synthesis of electropolymerized *N*-substituted methacrylamide matrices onto graphite fibers. These polymers have glass-transition temperatures greater than 200°C, which is desirable for moderate temperature composite applications.

In particular, the results from electropolymerized 2- and 4-carboxy phenylmethacrylamide (2- and 4-CPM)/methylmethacrylate (MMA) copolymers and 4-carboxyphenyl methacrylamide/N-phenylmaleimide (NPMI) copolymers will be discussed here. Properties of the unidirectional composites fabricated from the prepregs will be reported in a separate paper.

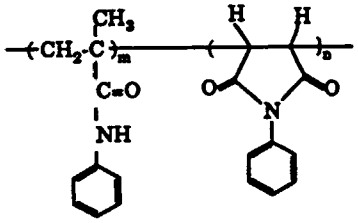

phenylmethacrylamide/phenylmaleimide copolymer
(PM/NPMI copolymer)

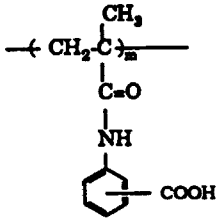

2- or 4- carboxyphenylmethacrylamide homopolymer
(2- or 4- CPM homopolymer)

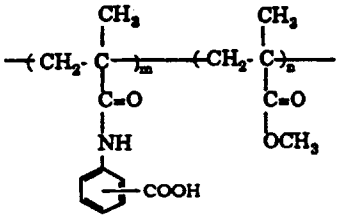

2-or 4-carboxyphenylmethacrylamide/methylmethacrylate copolymer (2- or 4- CPM/MMA copolymer)

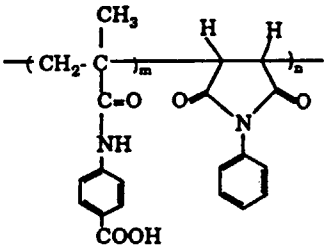

4-carboxyphenylmethacrylamide/N-phenylmaleimide copolymer (4- CPM/NPMI copolymer)

Figure 1 Chemical structures of the electropolymerized polymer systems.

EXPERIMENTAL

Materials and Electropolymerization

2- and 4-carboxyphenyl methacrylamide (2-CPM and 4-CPM) (Fig. 1) were synthesized by condensation of methacryloyl chloride (from Monomer & Polymer Lab, Inc.) with 2- or 4-aminobenzoic acid (from Aldrich Chemical Co.) following a published procedure.[17] The melting points were found to be 177°C for 2-CPM and 227°C for 4-CPM. Phenylmethacrylamide and phenylmaleimide (from Monomer & Polymer Lab., Inc.) were used as received. MMA was distilled under reduced pressure and kept cold. *N*-Phenylmaleimide (NPMI) (from Mitsui Toatsu Chemical Inc., Japan) was used as received. 4-Carboxyphenylmaleimide (4-CMI) was synthesized according to the method of Sauers[18] using reagent-grade ingredients.

Electropolymerization was done at room temperature by a published method[10]: a 3000-filament AS-4 graphite fiber bundle (from Hercules, Inc.) was wound onto a polypropylene H-frame (6 cm × 12 cm). This H-frame with 2 g of fibers was put into the central chamber of a three-compartment cell.[11]

This central chamber contained monomer and sulfuric acid electrolyte dissolved in dimethylacetamide and water solution. The reaction was controlled by passing a constant current of 30 mA/g of fiber through the cell, using the graphite fiber as cathode and metal anodes (tantalum oxide coated with magnesium oxide, DSA®4158-IT, Eltech System Co.) in the two outer compartments. The outer compartments were separated from the fibers by a polypropylene membrane (SEPA®YB01, Osmonic, Inc.). Electropolymerization was carried out until a weight gain of 35% (67% fiber volume fraction) was attained (20 min to 7 h). At the end of the electropolymerization, the graphite fibers were removed from the solution, rinsed thoroughly with DMAc/water mixture to remove the monomer residue and dried at room temperature. The weight gain on the graphite fibers was obtained by weighing the sample after drying for 2 h at 250°C in vacuum. No weight loss caused by residual DMAc was found by a Perkin–Elmer thermogravimetric analysis (TGA) at a heating rate of 30°C/min under a nitrogen environment.

Electropolymerization was also conducted at temperatures of 35°C and 45°C for 4-CPM/MMA, 4-CPM/4-CMI and 4-CPM/NPMI.

Characterization

Cyclic Voltammetry

The electroactivities of the monomer, solvent, and electrolyte were monitored by cyclic voltammetry. A BAS-100 electrochemical analyzer manufactured by Bioanalytical Systems, Inc. was used. Glassy carbon was used as the working electrode. A platinum electrode and an electrode of Ag/AgCl (saturated KCl) were used as the counter and reference electrodes, respectively. A potential sweep with reversal between −3.0 V and 0.0 V was applied at a cathodic sweep rate of 100–250 mV/s.

UV Spectroscopy

Ultraviolet absorption spectra of diphenylpicrylhydrazyl (DPPH), a radical scavenger, were collected to monitor the generation of monomeric free radicals by the reduction of monomers in the catholyte solution. The percentage of unreacted DPPH was calculated using an absorbance vs. concentration calibration curve. A 20 μL sample of the reaction solution was taken into a reaction vial after electrolysis at constant potential for a given time, and then was diluted with DMAc to $10^{-5}M$ for UV measurements. Ultraviolet spectra from 250–900 nm wavelength were recorded on a Perkin–Elmer Lambda Array 3840 UV/Vis Spectrophotometer.

CV/FTIRS

FTIR *in situ* multiple internal reflection Fourier transform infrared spectra (FTIRS) were recorded during polymerization using a Nicolet 60SX Fourier transform spectrometer and following a published procedure.[19] A spectroelectrochemical cell was designed according to the description of Pham, Adami, and Dubois.[20] A germanium crystal (50 mm × 20 mm × 2 mm with an incidence angle of 45°) was used as both reflection element and working electrode. The reference electrode was made from AgCl/Kel-F800 and the counterelectrode was a platinum plate. *In situ* FTIRS spectra of adsorbed species at an indicated potential on the electrode surface are reported here as absorbance difference spectra; for each spectrum of a series, the absorbance spectrum of the electrode/electrolyte solution before polarization was subtracted from that of the reacting system at an indicated voltage. The scale factors for subtraction are the same for all spectra of a series. The potential scan rate of 5 mV/s was programmed using an EG&G model 362 scanning potentiostat.

Phase Diagram

Ternary phase diagrams were determined by preparing mixtures of either polymer or monomer with DMAc/water at a given ratio in 20 mL vials. All samples were thermostated using a water bath at 30°C for at least 3 days, after which time the samples were visually judged to be one-phase isotropic solutions at 30°C. This procedure was repeated until turbidity was observed, thus establishing a series of points on the phase diagram.

Diffusion and Mass Transfer Evaluation

The diffusion of active species through swollen polymer films was studied by measuring the electrochemical behavior of the hexacyanoferrate(III)/ferrate(II) couple using a polymer-coated glassy carbon electrode with a tip diameter of 4 mm. A similar technique was applied to surface-oxidized graphite fibers by Porter et al.[21] The thickness of dry film on the glassy carbon electrode was estimated by calculation from polymer weight gain and polymer density. The experiments were performed by immersing the uncoated and polymer-coated glassy carbon electrode in a 40 mM solution of potassium

hexacyanoferrate(III) in 1*M* KCl. All potentials were measured with respect to an Ag/Ag^+ reference electrode.

Coating Morphology

Surface morphology of the polymer-coated graphite fibers was examined by scanning electron microscopy (SEM). Both an Amray 1000A and an Amray 1200B SEM were utilized. The polymer-coated graphite fibers after removal from the electrochemical cell were freeze-dried and coated by sputtering with a thin layer of gold to avoid charging effects. First, a polymer-coated graphite fiber bundle was cut into a length of 2 cm immediately after removal of the fibers from the electropolymerization cell. This short fiber bundle was then dropped into a liquid nitrogen bath. The frozen fiber bundle was dried by application of vacuum for 5 h inside a test tube immersed in a liquid nitrogen bath.

Copolymer Composition Determination

IR spectra were recorded on a Nicolet FTIR spectrometer, from pellets containing polymer that was crushed and dispersed in KBr. These spectra were used to determine the 2-CPM/MMA, 4-CPM/MMA, and 4CPM/NPMI copolymer compositions, and were based on calibration curves from known mixtures of the four homopolymers. IR absorbances at 1726 cm^{-1} (ester carbonyl group) and 1519 cm^{-1} (amide carbonyl group) were chosen for polymethylmethacrylate and polycarboxyphenyl methacrylamide, respectively. IR absorbances of 1772 cm^{-1} (imide carbonyl group) and 1519 cm^{-1} were selected for polyphenylmaleimide and polycarboxylphenyl methacrylamide, respectively.

^1H NMR spectra of the 4CPM/MMA copolymers were taken in DMSO-d_6 solution (0.4 wt %) on a Bruker AC-270 spectrometer operating at 270 MHz. Tetramethylsilane (TMS) was used as an internal standard. The 4CPM/MMA copolymer composition of each sample was also calculated from ^1H NMR spectroscopy by following a published procedure.[22]

Molecular Weight Measurement

Gel permeation chromatography (GPC) was done using a Waters model 150-C instrument with Ultrastyragel-HT columns (pore size of 10^5, 10^4, 10^3, 500, and 100 Å) in dimethylacetamide at 70°C. Number and weight-average molecular weights ($\overline{M}_{n\mathrm{GPC}}$ and $\overline{M}_{w\mathrm{GPC}}$) were calibrated with standard narrow-distribution polystyrene samples, and it was assumed that the polystyrene calibration curve was approximately applicable to the polymers tested.

Thermal Analysis

Glass-transition temperatures of composites were obtained by dynamic mechanical analysis (DMA) using a Polymer Laboratories DMTA at 1 Hz and heating rate of 5°C/min. The T_g of the polymer matrix was determined by differential scanning calorimetry (DSC) at a heating rate of 15°C/min. Thermal stability was characterized by a Perkin–Elmer TGA instrument at a heating rate of 30°C/min under a nitrogen environment.

RESULTS AND DISCUSSION

The chemical structures of electropolymerized *N*-substituted methacrylamide matrices that have been successfully electropolymerized onto graphite fibers were shown in Figure 1. Although all of the structures have bulky, stiff groups in each repeat unit, data from Table I shows that the rate of polymer weight gain and T_g are highly dependent upon the type of monomer or comonomer used. Due to the stiff side chains and a considerable degree of hydrogen bonding between the amide and acid groups along the polymer chains, all of the polymers have T_g's above 200°C. A comparison of the selected reaction time and weight gain data (Table I) shows that only the 2-CPM/MMA, 4-CPM/MMA, 4-CPM/PMI, and 4-CPM/4-CMI copolymers were deposited at a high rate of polymerization at room temperature.

The criteria for obtaining a thick coating on graphite fibers require not only that the monomer polymerize rapidly but also require that the polymer formed on the graphite fibers swells sufficiently to allow monomer to diffuse through easily. When diffusion is rapid, the polymer coating can grow thicker in a short time. A high diffusion rate may be the reason for the observed high rate of weight gain for (2-CPM or 4-CPM)/MMA and 4-CPM/PMI, or the reason may relate to steric hindrance of the bulky monomers when used singly. The intrinsic viscosities, $[\eta]$, of 2-CPM and 4-CPM are a little lower than the values found for 2-CPM/MMA or 4-CPM/MMA, but the difference is not great (Table I). If the rate of initiation remains constant and the rate of polymerization is relatively low for 2-CPM or 4-CPM, the corresponding number average molecular weights and $[\eta]$ should also be low. Since the

Table I Effects of Monomer Structure on Polymer Weight Gain and T_g

Monomer	Reaction Condition: Monomer Conc. (M/L)	Reaction Condition: Current Density (ma/g fiber)	Reaction Condition: Reaction Time (h)	Wt. Gain[a] (%)	T_g (°C)	$[\eta]$[d] (dL/g)
PM/NPMI	0.5	30	9	40	220[b]	0.50
2-CPM	0.5	30	7	40	250[c]	0.61
4-CPM	0.5	30	7	45	300[c]	0.68
2-CPM/MMA	0.5	30	0.5	35	210[b]	0.75
4-CPM/MMA	0.5	30	0.5	40	240[b]	0.81
4-CPM/4-CMI	0.5	30	3	35	235[b]	—
4-CPM/NPMI	0.5	30	3	43	225[b]	—

[a] 35% weight gain, ~67% fiber volume fraction calculated by using density of 1.8 g/cm^3 for fibers and density of 1.18 g/cm^3 for matrices.

[b] T_g depends on polymer composition:
0.45 mole fraction of PM in PM/MI copolymer (T_g ~ 220°C)
0.5 mole fraction of 2-CPM in 2-CPM/MMA copolymer (T_g ~ 210°C)
0.49 mole fraction of 4-CPM in 4-CPM/MMA copolymer (T_g ~ 240°C)
0.47 mole fraction of 4-CPM in 4-CPM/4-CMI copolymer (T_g ~ 235°C)
0.44 mole fraction of 4-CPM in 4-CPM/NPMI copolymer (T_g ~ 225°C)

[c] These values were attained after reheating the sample in DMTA.

[d] In dimethylacetamide at 30°C.

molecular weights are not low, the data seem to indicate that diffusion is limiting.

Because of the ease of electropolymerization and high T_g, the CPM/MMA and CPM/PMI systems were fabricated into composites. Their properties are discussed in a separate paper.

Reaction Mechanism

The reduction peak potentials, from cyclic voltammetry, of active species are tabulated in Table II. Sulfuric acid, methylmethacrylate, 2-CPM, and 4-CPM have relatively high reduction peak potentials of −2.3, −2.4, −2.7, and −2.6 V, respectively. Table II shows that a low reduction peak of −1.9 V emerged for 4-CPM/MMA or 2-CPM/MMA mixtures, lower than the original reduction peak of −2.6–−2.7 V for 4-CPM or 2-CPM alone. Some kind of interaction between CPM and MMA monomers must have facilitated the reduction potential when both were present. Phenylmaleimide and 4-carboxyphenyl maleimide alone have lower reduction potentials of −1.7 V and −1.6 V, respectively. These reduction potentials decreased further to −1.3 V when both the maleimide and styrene were present. DPPH was electro-inactive until a potential of −2.6, where a low amount of reduction occured.

Table III shows polymer weight gain vs. reaction time for different monomer or comonomer systems at room temperature. It was found that the electropolymerization rate was slow for either 2-CPM or 4-CPM alone; for a long electropolymerization time of about 7–9 h, a high polymer weight gain of 50% was obtained for both. However, a 2-CPM or 4-CPM monomer mixture with methylmethacrylate was electropolymerized easily to give a high polymer weight gain in a short reaction time. A large increase

Table II Reduction Potentials of Active Species

Active Species	Reduction Potential (V)	Remark
Water	> −3.0	Solvent
DMAc[a]	> −3.0	Solvent
TBAP[b]	> −3.0	Electrolyte
H_2SO_4	−2.30	Electrolyte
DPPH[c]	−2.60	Radical scavenger
MMA	−2.40	—
4-CPM	−2.60	−1.90, −2.60 for 4-CPM/MMA mixture
2-CPM	−2.70	−1.90, −2.70 for 2-CPM/MMA mixture
NPMI	−1.70	—
4-CMI	−1.60	—

[a] Dimethylacetamide.

[b] Tetrabutylammonium perchlorate.

[c] Diphenylpicrylhydrazyl.

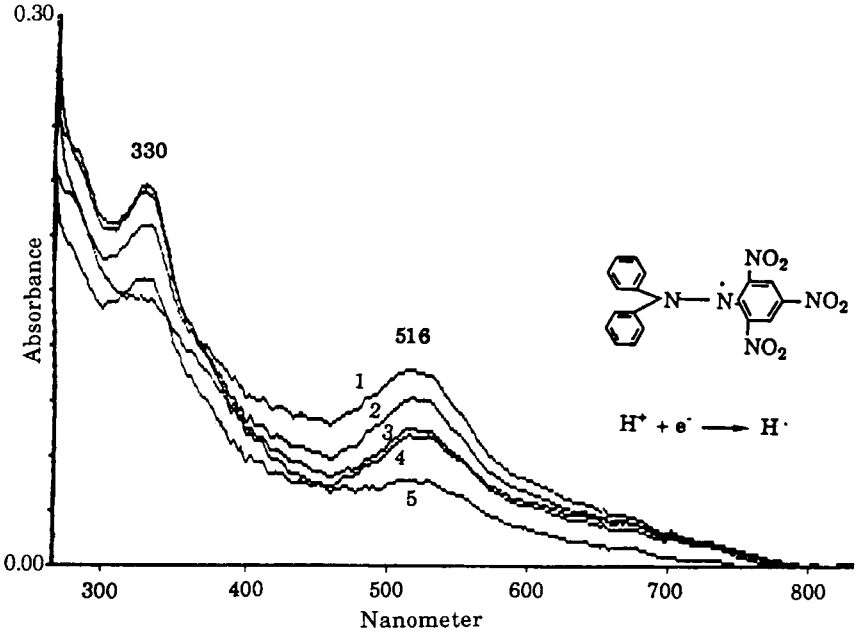

Figure 2 The UV absorbance of DPPH at 516 nm decreases as a function of electrolysis time at a constant potential of −2.0 V in the presence of 0.0125 *M* sulfuric acid electrolyte: (1) 0 min, (2) 10 min, (3) 20 min, (4) 30 min, (5) 120 min.

in weight gain was also observed for the electropolymerization of 4-CPM/NPMI or 4-CPM/4CMI mixtures. This phenomenon was investigated in terms of reaction mechanism and other parameters such as diffusion and monomer reactivity.

The concentration of added DPPH, indicated by UV absorbance at 515 nm, decreased (Fig. 2) during electrolysis of hydrogen ions (from the H_2SO_4 electrolyte) at a constant potential of −2.0 V. The decrease was caused by the generation of hydrogen radicals by reduction of hydrogen ions from the electrolyte, and the capture of these radicals by DPPH. Radicals from sources other than hydrogen ions from the electrolyte have also been detected, such as from the reduction of MMA when tetrabutylammonium perchlorate (TBAP) electrolyte was present (Fig. 3). Only the lowest curve in Figure 3 represented an electrolysis experiment that used a H_2SO_4 electrolyte. A TBAP electrolyte without a reduction below −3.0 V was used in the other electrolysis experiments (Fig. 3).

MacCallum and Mackerron[23] reported that MMA could be electropolymerized onto graphite fibers; the polymerization followed a typical free-radical mechanism. We found that the rate of consumption of DPPH was somewhat slower for MMA radicals than hydrogen radicals (Fig. 3). This is perhaps caused by the steric hindrance of the larger MMA radicals, making the reaction with DPPH more difficult. However, the stability and efficiency of MMA radicals, once they were generated, was demonstrated by an increased rate of polymer weight gain (Table III). The rate of generation of polymer initiated by hydrogen radicals was low in either 2-CPM or 4-CPM alone. This lower efficiency is possibly caused by the recombination of hydrogen radicals to form hydrogen gas and/or possibly a low polymerization rate of the homopolymers because of steric hindrance between monomer units. However, other factors such as low diffusion rates of species through these polymers can not be ruled out. An initiation efficiency from 0.018 to 0.27 for the electropolymerization of acrylamide has been reported by Iroh, Bell, and Scola.[13]

Phenylmaleimide was difficult to electropolymerize alone, although this monomer was easily polymerized with a thermal-induced initiator at 60°C.[24] However, the interaction of phenylmaleimide and 4-CPM did promote radical generation (Fig. 3) and the formation of high polymer by electropolymerization (Table III). It seems that the two monomers preferentially copolymerize rather than homopolymerize.

CV/FTIRS Investigation

CV/FTIRS spectra during electropolymerization on germanium were monitored by *in situ* FTIRS. No

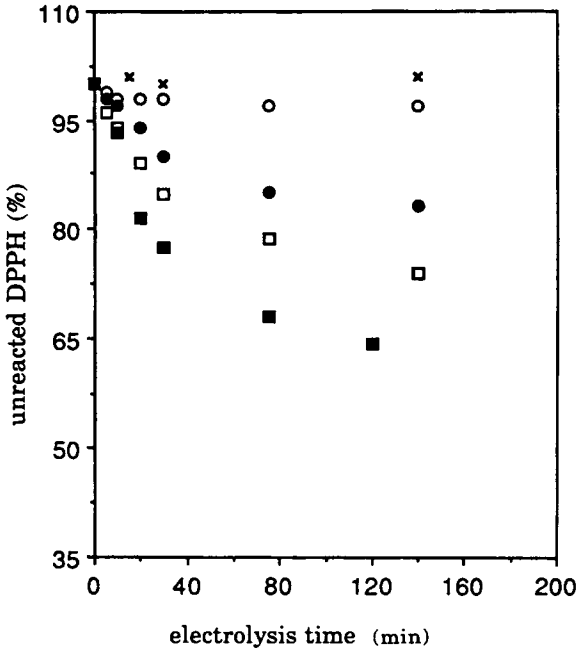

Figure 3 The DPPH consumption changes as a function of electrolysis time at −2.0 V for different active species, (×) DPPH/TBAP; (○) DPPH/4-CPM/TBAP; (●) DPPH/4-CPM/NPMI/TBAP; (□) DPPH/MMA/TBAP; (■) DPPH/0.0125*M* sulfuric acid solution.

electropolymerization to form polymer, as indicated by changes in the spectra, was observed for 2-CPM or 4-CPM monomer alone (not shown). On the other hand, formation of polymethylmethacrylate from MMA was detected at a potential of −2.0 V on germanium (Fig. 4). Furthermore, both the 4-CPM/MMA mixture and the 4-CPM/NPMI mixture were easily electropolymerized onto the germanium electrode. The characteristic bands of polymethylmethacrylate (ester carbonyl, 1726 cm^{-1}) and polymethacrylamide (amide carbonyl, 1515 cm^{-1}) were detected at a potential of −2.0 V (Fig. 5) and increased gradually. Figure 6 shows that the IR absorbance of polymaleimide (imide carbonyl, 1710 cm^{-1}) and polymethacrylamide (amide carbonyl, 1515 cm^{-1}) appeared at a potential of −2.1 V, and increased gradually with voltage. Based on the combined data of the weight gain, DPPH consumption, and CV/FTIRS spectra, initiation by free radicals can occur both due to formation of hydrogen radicals, or to monomer or monomers adduct reduction to give radicals. Similar reaction mechanisms have been proposed by MacCallum and Mackerron,[23] and Iroh, Bell, and Scola.[11]

Table IV shows that the 4-CPM/MMA copolymer composition (represented by the 1515 cm^{-1}/1726 cm^{-1} ratio) during constant potential electrolysis does not change appreciably with times to 180 s at a fixed monomer feed ratio. This result infers that the monomer ratio in both polymer and bath remained nearly constant at a low monomer conversion. Monomer conversion was estimated at less than 5%, using the weight gain of polymer formed on the germanium electrode. However, the copolymer composition did depend upon monomer feed ratio (Table IV). The same trend was also found for the polymer composition of 4-CPM/NPMI (Table IV). These data demonstrate that although interaction between comonomers did increase the electropolymerization rate for both systems, the individual monomers still polymerized more or less randomly. This is in contrast to the 4-carboxyphenylmaleimide/styrene system, where the interaction between styrene and maleimide not only increased the reaction rate but also caused the formation of an alternating copolymer.[11]

Table III Polymer Weight Gain (wt %) as a Function of Time for Different Monomer Systems at Room Temperature

	Electropolymerization Time (min)			
Monomer System[a]	10	20	30	60
2-CPM	0.30	0.37	1.14	2.53
4-CPM	0.52	1.15	1.58	3.23
2-CPM/MMA (50 : 50)[b]	10.1	22.1	30.7	50.4
4-CPM/MMA (50 : 50)	12.7	25.5	38.2	57.1
4-CPM/NPMI (50 : 50)	1.51	3.04	4.52	9.08
4-CPM/4-CMI (50 : 50)	1.73	3.35	4.70	9.51

[a] DMAc/water ratio: 60/40; curernt density: 30 mA/g of fiber; H_2SO_4 conc.: 0.0125*M*
[b] Monomer molar ratio.

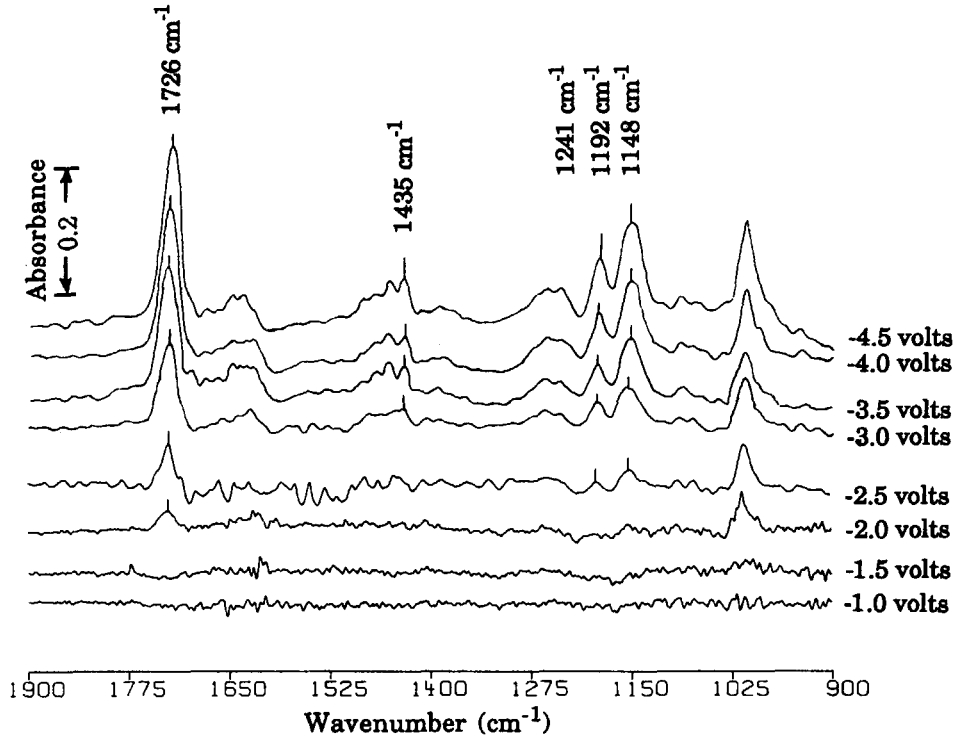

Figure 4 CV/FTIRS spectra of MMA change on a germanium electrode as a function of applied voltages.

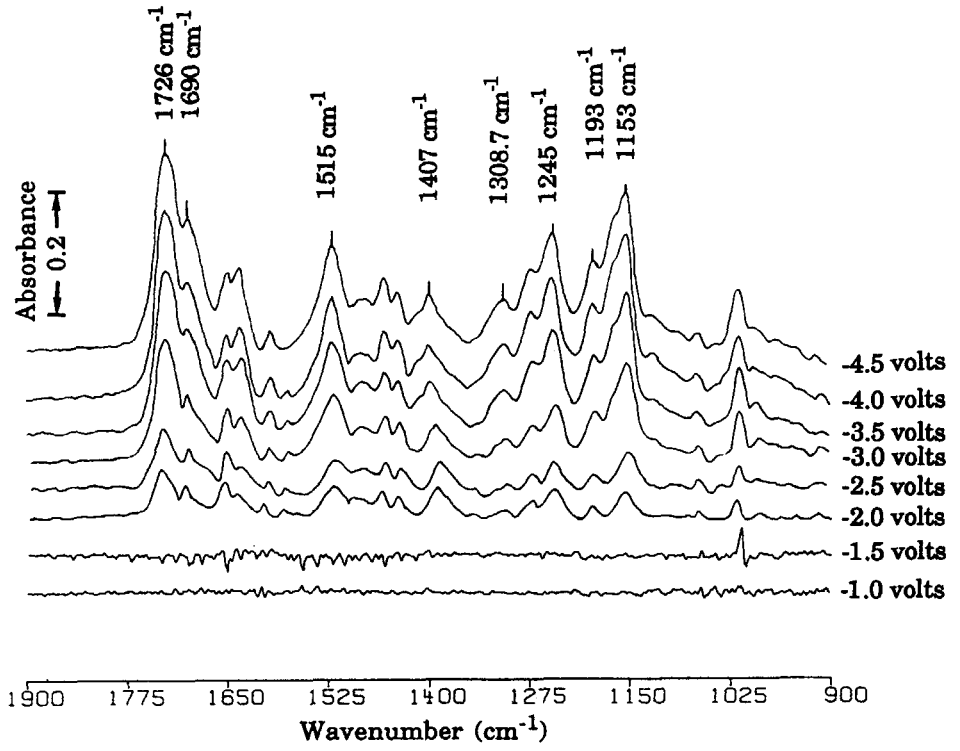

Figure 5 CV/FTIRS spectra of 4-CPM/MMA change on a germanium electrode as a function of applied voltages.

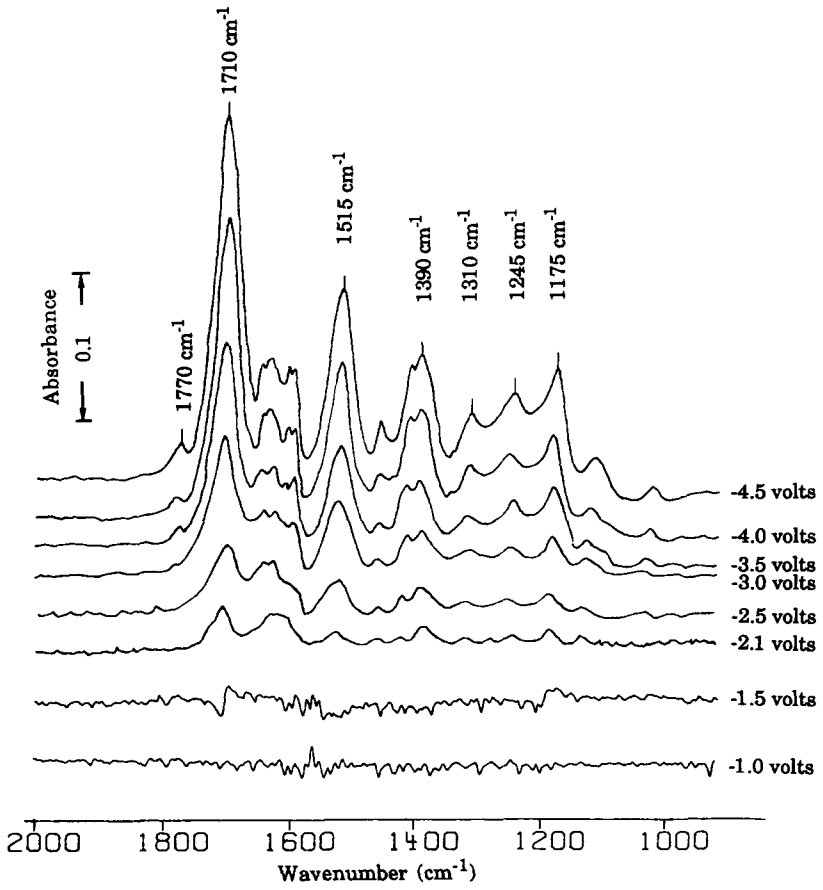

Figure 6 CV/FTIRS spectra of 4-CPM/NPMI change on a germanium electrode as a function of applied voltages.

Coating Morphology

Excellent wetting is observed by comparison of uncoated (7.2 μm diameter) and polymer-coated single graphite fibers (Fig. 7). A tight, even-thickness polymer film was formed tightly on the smooth fiber surfaces [Figs. 7(2,3)]. Nodular structures [Fig. 7(2)] could perhaps have resulted from the coalescence and the aggregation of polymer chains during the freezing process or could have been present in the polymer as formed. After removing the top polymer layers by rigorously shaking, very fine nodular structures of 0.1 μm were found underneath [Fig. 7(3)]. Some larger nodular particles were still found on the fiber surfaces.

Table IV Intensity Variation of CV/FTIRS Spectra During Constant Potential Electrolysis

Time (s)	4-CPM/MMA (1515 cm^{-1}/ 1725 cm^{-1}) 60/40	4-CPM/MMA (1515 cm^{-1}/ 1725 cm^{-1}) 40/60	4-CPM/NPMI (1515 cm^{-1}/ 1710 cm^{-1}) 80/20	4-CPM/NPMI (1515 cm^{-1}/ 1710 cm^{-1}) 70/30
84	0.81	0.52	0.70	0.53
108	0.78	0.56	0.75	0.49
132	0.84	0.50	0.72	0.50
156	0.81	0.54	0.69	0.52
180	0.79	0.56	0.73	0.49

Polymer Swelling and Morphology

As soon as polymer is formed, the electrical resistivity of the cell increases, radicals have greater difficulty diffusing outward and monomers have greater difficulty diffusing inward through the polymer layer toward the electrode surfaces. This behavior can be minimized to continually promote polymer growth by adequate solvent swelling. Therefore, the water/DMAc ratio was optimized to promote the diffusion of monomers and free radicals without dissolving the polymer.

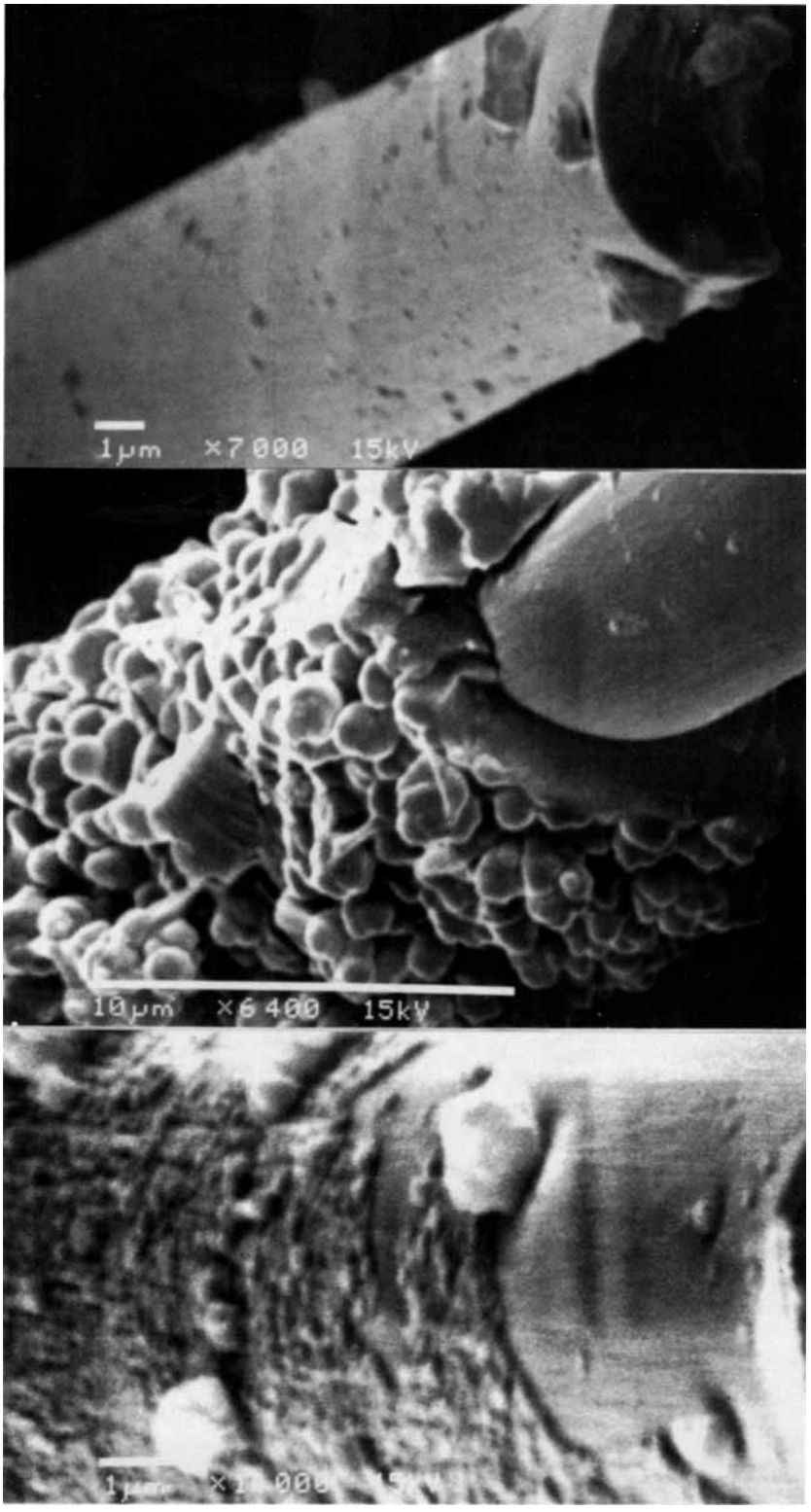

Figure 7 SEM micrographs of (1) a single graphite fiber, (2) 4-CPM/MMA polymer-coated graphite fiber, and (3) fine nodular polymer particles on graphite fiber surfaces.

A phase diagram of 4-CPM/MMA monomers and copolymer was constructed to investigate the solvent-swelling effect on polymer growth. The precipitation boundary lines of 4-CPM monomer and 4-CPM/MMA copolymer are shown in Figure 8. There are four starting DMAc/water molar ratios: 40/60, 55/45, 65/35, and 90/10, respectively. On Figure 8, lines have been drawn to differentiate areas of different behavior 1, 2, 3, and 4.

In the region of monomer precipitation (Fig. 8, area 1), all of the fiber surfaces were covered with monomer crystals and no polymer weight gain was found after extracting the monomer-coated fibers. By increasing the DMAc/water ratio slightly over the monomer precipitation boundary (Fig. 8, area 2), number average molecular weight ($\overline{M_n}$) and polymer weight gain were about 7.3×10^4 and 27%, respectively. When the DMAc/water ratio was further increased 65/35 (Fig. 8, area 3), $\overline{M_n}$ and polymer weight gain increased to 8.7×10^4 and 38%, respectively. When the DMAc/water ratio crossed the polymer precipitation boundary (Fig. 8, area 4), a 3% polymer weight gain was found on the graphite fibers. The explanation is likely due to the rate of polymer dissolution into solution being faster than the rate of polymer generation.

As shown on Table I, 2- and 4-CPM/MMA have similar polymerization rates. The polymer weight gain for the 2-CPM/MMA system presented the same trend.

Diffusion Investigation

The electrochemistry of a polymer-coated glassy carbon electrode was investigated to provide additional information concerning the role of diffusion of radicals and monomers. The cyclic voltammetry of Fe(II)/Fe(III) was studied for uncoated and polymer-coated glassy carbon electrodes dipped in a given DMAc/water/KCl solution.

A series of voltammograms of the hexacyanoferrate(III)/ferrate(II) couple in DMAc/water/KCl electrolyte solution at different voltage scanning rates are shown in Figure 9. Scan rates between 1 mV/s and 10 mV/s were used to calculate the diffusion coefficient of the hexacyanoferrate(III) ion. Under these conditions reversibility is maintained; the areas under the oxidation and reduction peaks, representing the charge involved, are essentially equal for uncoated and polymer-coated glassy carbon electrodes at a given scanning rate. The diffusion coefficient of hexacyanoferrate(III) ion may be determined by measuring the peak height (here the reduction scan is used), i_{red}, and using the following equation[25]:

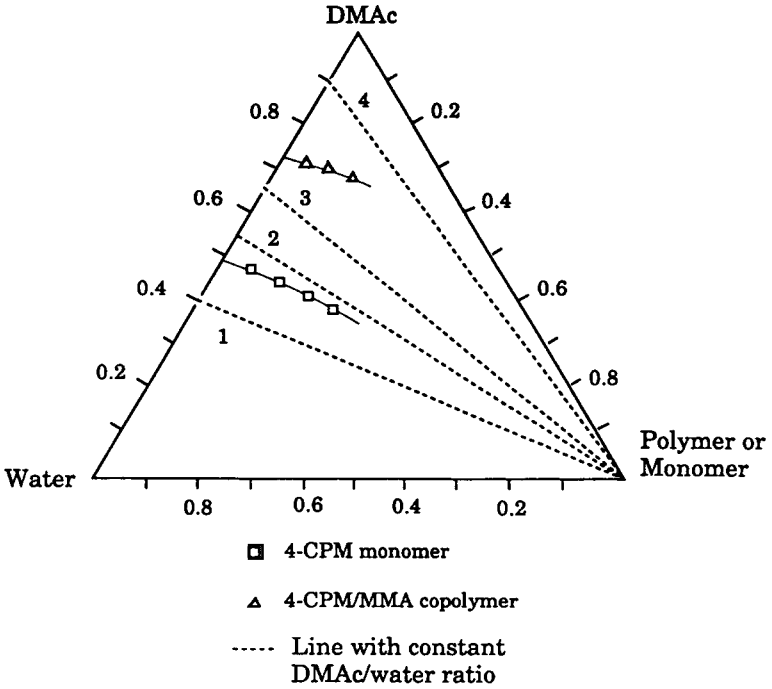

Figure 8 Phase diagram of 4-CPM/MMA monomer pairs, 4-CPM/MMA copolymer, DMAc solvent, and water mixtures.

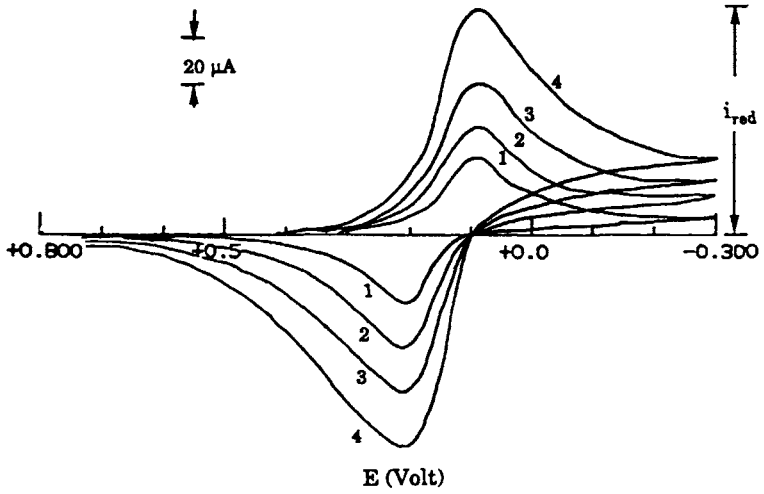

Figure 9 Cyclic voltammograms of $Fe(CN)_6^{-3}$ on the 4-CPM/MMA copolymer-coated glassy carbon electrode in the presence of 1 *M* KCl electrolyte at (1) 1 mV/s; (2) 2 mV/s; (3) 4 mV/s; and (4) 8 mV/s.

$$i_{red} = 2.69 \times 10^5 n^{3/2} A \cdot C \cdot D^{1/2} v^{1/2} \quad (1)$$

where D is the diffusion coefficient (cm^2/s), A is the surface area of the electrode (cm^2), C is the concentration of hexacyanoferrate(III) ion (4×10^{-5} mol/cm^3), n is the number of electrons transferred (1), and v is the scan rate (V/s). A slope for determining the D value was obtained by plotting a graph of i_{red} against $v^{1/2}$ (not shown).

The D values of hexacyanoferrate(III) ion in the presence of uncoated and 4-CPM/MMA polymer-coated glassy carbon electrodes are tabulated in Table V. The D values of the uncoated electrode at three different DMAc/water ratios changed slightly; the D values were around 50% less than in pure water medium. The change could possibly be caused by the DMAc viscosity effect on the diffusion coefficient. However, a dramatic drop of D values was found after application of a 1.11-μm thickness 4-CPM/MMA polymer coating on the electrode. The average drop of one order of magnitude indicated that the diffusion or mass transfer of active species quickly changed as soon as the first thin polymer layer was generated and coated on the electrode surfaces. When the layer thickness was doubled, the D value dropped even further. While there is a drop in D of nearly an order of magnitude on coated samples, it is clear that the relatively large hexacyanoferrate ions are still "getting through" and diffusion of monomers to the conductive surface is not prohibited, nor diffusion of radicals outward.

Table V Diffusion Coefficient of Hexacyanoferrate(III) Ion Through Uncoated and 4-CPM/MMA Polymer-Coated Glassy Carbon Electrodes

Coating Thickness (μm)	DMAc/Water Volume Ratio ($D \times 10^6$, cm^2/s)			
	0/100	53/47	60/40	65/35
0	6.02	4.31	4.18	3.95
1.11	—	0.46	0.61	0.82
2.35	—	0.27	0.42	0.61

By increasing the amount of solvent for swelling the polymer, the D value increased substantially (Table V). This increase enhances the diffusion rate of active species. The high diffusivity infers that most of the polymer chains were highly swollen. These data imply that the diffusion of hexacyanoferrate(III) ions is directly through the polymer layer, which can be though of as a viscous liquid layer swollen with solvent and supporting electrolyte ions on the surface of the electrode. Peerce and Bard[26] have investigated the redox behavior of thianthrene using electrodes coated with poly(vinylferrocene) films. A strong dependence of the cyclic voltammetric behavior of thianthrene on the thickness of films was found in their study. They concluded that diffusion of the reactant through the polymer layer to the underlying substrate material occurs via diffusion through the polymer layer, viewed as a homogeneous medium, and through tortuous channels of larger-than-molecular diameters in the film.

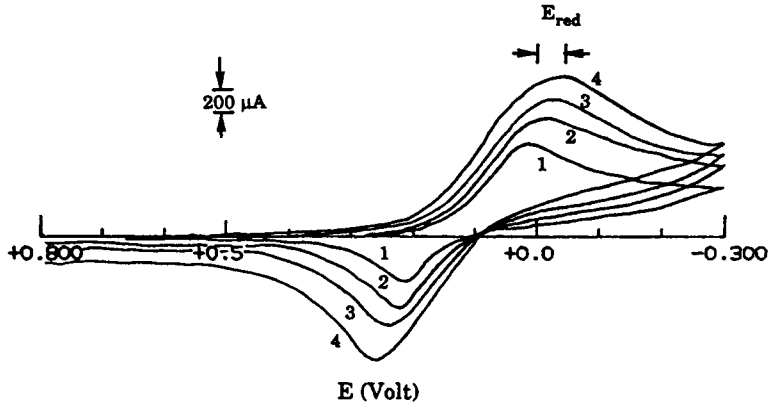

Figure 10 Cyclic voltammograms of $Fe(CN)_6^{-3}$ on the 4-CPM/MMA copolymer-coated glassy carbon electrode in the presence of 1*M* KCl electrolyte at (1) 100 mV/s; (2) 150 mV/s; (3) 200 mV/s; and (4) 250 mV/s.

Data related to the ease of electron transfer across the glassy carbon–polymer interface can be obtained by plotting the peak reduction potential, E_{red} (see Fig. 10), against $\log_{10}[v]$, where v is the scan rate in V/s. At higher scan rates the value of E_{red} becomes dependent on the scan rate as the electrochemical reaction becomes more irreversible. E_{red} can be expressed by the relationship.[27]

$$E_{red} = E_{const} - 2.303RT \log[v]/2\partial NF \quad (2)$$

where E_{const} is a constant, F is Faraday's constant, R is the gas constant, and N is the number of electrons transferred in the rate-limiting step. The term ∂ is the transfer fraction related to the effect that the applied potential has on the activation energy of the rate-limiting step. A fall in ∂N means that the reduction becomes a more difficult to achieve. Table VI shows the transfer coefficient of hexacyanoferrate(III)/ions at different DMAC/water ratio with uncoated and polymer-coated electrodes. The value of ∂N decreased for the polymer-coated electrodes of both 1.11-μm and 2.35-μm thickness. In general ∂N values for the high DMAc/water ratio are higher than those measured for the low DMAc/water ratio.

Table VI The Transfer Coefficient ∂N of Hexacyanoferrate(III) Ion on Uncoated and 4-CPM/MMA Polymer-Coated Glassy Carbon Electrodes

Coating Thickness (μm)	DMAc/Water Volume Ratio		
	53/47	60/40	65/35
0	0.552	0.543	0.526
1.11	0.175	0.234	0.308
2.35	0.103	0.189	0.261

Both the changes in diffusion coefficient and ∂N may be related to changes in the mass transfer of the hexacyanoferrate(III) ion through the solvent-swollen polymer coating. Based on these results, the optimum swelling of the polymer plays an important though not crucial role to the success of generating a thick polymer coating on substrates using the electropolymerization process. Other factors, such as the electroactivity of the monomers and the chemical reactivity of the monomers, control the formation of polymer and should therefore be considered first.

Reaction Kinetics

Results of polymer composition analysis by IR and NMR methods are summarized in Table VII for 4-CPM/MMA copolymers, and by IR for 2-CPM/MMA and 4-CPM/NPMI copolymers. In the IR method for determining composition, the calibration curve was obtained by using homopolymer blends with different compositions by weight. The composition was next transformed to molar ratio using $\overline{M}_{nGPC}$. The $\overline{M}_{nGPC}$ of PMMA, 4-CPM homopolymer, and NPMI homopolymer were 28,500, 21,000, and 19,600 g/mole, respectively. The absorption bands for calibration were 1726 cm^{-1} (carbonyl absorption characteristic of PMMA) and 1519 cm^{-1} (amide absorption of 4-CPM). The absorption band at 1772 cm^{-1} (imide carbonyl absorption of NPMI) was used for calibration.

Table VII The Composition Analysis and Number Average Molecular Weight of Several Copolymers

Monomer System[a]	Mole Fraction of M_2 in Monomer Feed Ratio	Copolymer IR	Copolymer NMR	Polymer Weight Gain (30 min, wt. %)
4-CPM(M_1)/MMA(M_2)	0.40	0.43	0.41	39.1
4-CPM(M_1)/MMA(M_2)	0.50	0.54	0.53	36.9
4-CPM(M_1)/MMA(M_2)	0.60	0.64	0.61	32.0
4-CPM(M_1)/MMA(M_2)	0.70	0.77	0.75	28.1
2-CPM(M_1)/MMA(M_2)	0.45	0.50	—	33.9
2-CPM(M_1)/MMA(M_2)	0.50	0.58	—	30.7
2-CPM(M_1)/MMA(M_2)	0.80	0.82	—	26.3
2-CPM(M_1)/MMA(M_2)	0.90	0.91	—	20.5
4-CPM(M_1)/NPMI(M_2)	0.50	0.54	—	8.95
4-CPM(M_1)/NPMI(M_2)	0.70	0.73	—	6.24
4-CPM(M_2)/NPMI(M_2)	0.90	0.91	—	4.53

[a] Monomer conc.: 0.5*M*; DMAc/water ratio: 60/40; current density: 30 mA/g of fiber; H_2SO_4 conc.: 0.0125*M*; all polymerizations were at room temperature.

In the ^{1}H-NMR spectra, the $-OCH_3$ group of MMA and the phenyl group of phenylmethacrylamide appeared around 3.8 ppm and from 7.0–8.0 ppm, respectively; these were used for composition analysis. The compositions of the copolymers were determined from the integrated proton NMR spectra by comparing the area of the $-OCH_3$ peak for MMA to the area of the phenyl peak for phenylmethacrylamide. From the copolymer structure, the following expressions were derived:

$$A_{C_6H_4} \propto 4 \text{ (no. 4-CPM units in chain)}$$

$$A_{OCH_3} \propto 3 \text{ (no. MMA units in chain)}$$

in which $A_{C_6H_4}$ and A_{OCH_3} are the integrated areas of the $-C_6H_4$, and the $-OCH_3$ protons, respectively. If n is the molar ratio (4-CPM/MMA) in the copolymer, then:

$$A_{C_6H_4}/A_{OCH_3} = 4n/3 \qquad (3)$$

for 4-CPM/MMA copolymers.

The data obtained by these IR and NMR methods for the composition of the 4-CPM/MMA samples (Table VII) are in close agreement.

The monomer reactivity ratios (r_1, r_2) of 4-CPM/MMA and 2-CPM/MMA were obtained by using the Fineman–Ross method.[28] The values of $r_{1,4\text{-CPM}}$ and $r_{2,MMA}$ for 4-CPM/MMA were determined to be 0.67 and 1.37, respectively. The high reactivity ratio for MMA indicated that the copolymer would be expected to contain somewhat more MMA units relative to 4-CPM than the monomer solution. Table VII indicates a somewhat higher concentration of MMA in the polymer relative to the monomer. Because of the interaction of MMA radicals and 4-CPM monomer, the electropolymerization rate and the polymer weight gain of 4-CPM/MMA copolymer were both increased dramatically relative to the 4-CPM homopolymer. It is only when r_1 and r_2 do not differ markedly, in the 4-CPM/MMA case for example, that there will exist a large range of comonomer feed compositions that can yield copolymers containing appreciable amounts of both monomers.

For the 2-CPM/MMA system, $r_{1,2\text{-CPM}}$ and $r_{2,MMA}$ were 0.38 and 0.90, respectively. The same conclusion found for the 4-CPM/MMA system also applies to the 2-CPM/MMA system; the presence of the MMA radicals is the reason for the very high polymer yield in a short time; the 2-CPM monomer alone electropolymerized very slowly under the same reaction conditions. Polymer weight gains for 4-CPM/MMA were somewhat higher than those of 2-CPM/MMA at the same conditions (current density, monomer concentration, monomer feed ratio, and reaction time). It is postulated that a carboxyl group at the ortho position of the benzene ring leads to more steric hindrance and to more pronounced intramolecular H-bonding than a carboxyl group at the para position of the benzene ring. Similar behavior was reported by Patel, Desai, and Suthar[17] on the thermally initiated homopolymerization of 2- or 4-carboxyphenylacrylamide. They found that

the 2-carboxyphenyl acrylamide monomer polymerizes more slowly than 4-carboxyphenyl acrylamide monomer.

Table VII shows for 4-CPM/MMA and 2-CPM/MMA that the rate of polymer weight gain decreased with increasing MMA concentration. A more detailed discussion of this behavior will be given in a later section.

The $\overline{M_n}$, polydispersity, and composition analysis of 4-CPM/NPMI at three different monomer feed ratios are also presented in Table VII. For this monomer/comonomer system, $r_{1,4CPM}$ and $r_{2,NPMI}$ were 0.90 and 1.00, respectively. Both $\overline{M_n}$ and polymer weight gain were much lower than comparable values from the 4-CPM/MMA and 2-CPM/MMA systems. A higher steric hindrance for bulky phenylmaleimide against 4-CPM rather than that of flexible MMA may slow the electropolymerization rate. However, both the polymer weight gain and $\overline{M_n}$ increased by decreasing the NPMI concentration in the monomer feed. This will also be discussed further.

Although the interaction of NPMI and 4-CPM made the electropolymerization more rapid, it did not result in an alternating copolymer such as was observed for the copolymer generated from NPMI and styrene. In contrast, the copolymer of 4-CPM/NPMI was a random copolymer, according to the composition analysis of Table VII.

Electropolymerization rate, polymer weight gain, and $\overline{M_n}$ for a series of polymerizations of 4-CPM/MMA were determined as a function of reaction parameters such as time, current density, and monomer concentration. These results are summarized in Table VIII.

In general, the polymer weight gain increased with increasing electropolymerization time; $\overline{M_n}$ and polydispersity were about 80,000 and 3.0, respectively, not unusual values for free-radical polymerization, and similar to results found for electropolymerization of 3-CMI/styrene.[11]

Polymer weight gain or electropolymerization rate (wt %/min) increased with increasing current density, and a logarithmic plot of ln R_p (rate of polymerization) as a function of ln C_d (current density) is linear, with a slope of 0.58, that is, $R_p \propto C_d^{0.58}$. However, the $\overline{M_n}$ decreased as the current density increased, because of the increasing initiation rate.

Increasing the total monomer concentration at a given monomer feed ratio also increased the polymer weight gain and electropolymerization rate. It was found that electropolymerization rate is dependent upon the total monomer concentration to a power of 1.07, or $R_p \propto M^{1.07}$. $\overline{M_n}$ increased slightly with increasing monomer concentration as expected. Somewhat unexpectedly, the total monomer concentration and the current-density dependence of electrocopolymerization rate (to a power of 1.07 and 0.58, respectively) are similar to the values found in Iroh, Bell, and Scola's work[12,13] on electrohomopolymerization of acrylamide and electrocopolymerization of 3-carboxyphenyl maleimide and styrene.

It was found that the electropolymerization rate and $\overline{M_n}$ of 4-CPM/MMA increased with an increase in the amount of 4-CPM in the monomer feed (Table

Table VIII Kinetics Analysis of Electropolymerization of 4-CPM/MMA

Monomer Conc.[a] (M/L)	Feed Ratio (4 CPM : MMA)	Current Density (mA/g)	Reaction Time (min) 10	20	30	60	R_p (%[c]/min)	$\overline{M_n}$ ($\times 10^{-4}$ g/mol)	$\overline{M_w}/\overline{M_n}$
0.5	50 : 50	20	9.67	19.3	29.1	49.8	0.965	8.83	3.4
0.5	50 : 50	30	12.7	25.5	38.2	57.1	1.275	8.11	3.2
0.5	50 : 50	40	14.0	30.1	45.0	64.8	1.505	7.25	3.1
0.5	50 : 50	30	12.2	24.0	36.6	55.3	1.20	7.94	3.3
0.6	50 : 50	30	14.0	27.4	42.1	60.7	1.40	8.23	3.2
0.7	50 : 50	30	17.3	32.6	48.9	66.5	1.73	8.41	3.3
0.5	30 : 70	30	9.02	19.1	28.8	44.3	0.92	4.25	3.0
0.5	40 : 60	30	11.0	21.7	33.0	50.4	1.08	6.25	3.4
0.5	50 : 50	30	13.1	24.7	39.1	55.7	1.25	8.01	3.1
0.5	90 : 10	30	11.8	22.2	33.3	51.6	1.12	7.52	3.2
0.5	100 : 0	30	0.52	1.15	1.58	3.23	0.05	4.18[b]	3.4[b]

[a] H_2SO_4 conc.: 0.0125*M*.
[b] Reaction time of 7 h.
[c] (%) g of polymer per g of graphite fiber.

VIII). However, the electropolymerization rate dropped slightly at a 4-CPM/MMA monomer feed ratio of 90 : 10. As more 4-CPM is added, the rate must finally approach the slow rate of 4-CPM alone. Kojima et al.[31] reported similar data for thermally-initiated polymerization of 4-CPM/MMA in terms of polymer yield and intrinsic viscosity. However, no explanation was given in their work. Other dependences of copolymerization rate on the monomer feed ratio have also been reported. The copolymerization rate might be monotonously changed as monomer feed composition was changed[29]; it has also varied from increase to decrease as monomer feed ratio changed.[30] We conclude that there is precedent for the CPM/MMA polymerization rate data as a function of feed ratio, but not a verified explanation.

Electropolymerization rate, polymer weight gain, and $\overline{M_n}$ for 4-CPM/NPMI were also measured, to investigate the reaction kinetics. These results of electropolymerization are summarized in Table IX. At 28°C electropolymerization temperature and a given monomer feed ratio, polymer weight gain increased as expected with increasing reaction time. The electropolymerization rate, R_p, increased with an increase of the applied current density (Table IX). The order of dependence on current density for R_p was about 0.60, $R_p \propto Cd^{0.6}$. $\overline{M_n}$ decreased as expected with increasing current density. R_p increased with an increase of total monomer concentration at a given monomer feed ratio (Table IX). It was found that R_p depended on monomer concentration with an order of 1.26; $\overline{M_n}$ increased slightly with increasing monomer concentration.

A lower $\overline{M_n}$ value and lower polymer weight gain were found for the 4-CPM/NPMI system than for the 4-CPM/MMA system. It seems reasonable that the lower rate for 4-CPM/NPMI was principally attributable to the steric effect being greater in the chain propagation of 4-CPM/NPMI than that of the 4-CPM/MMA, since MMA is a more flexible spacer in the polymer chain. Table IX shows that the electropolymerization rate and $\overline{M_n}$ for 4-CPM/NPMI increased dramatically with an increase in the amount of 4-CPM in the monomer feed ratio (Table IX, tests 7–9), but the electropolymerization rate was relatively constant between feed ratios of 90 : 10 and 95 : 05 for 4-CPM/NPMI. The polymerization rate must eventually drop to a low value, because of the fact that 4-CPM alone electropolymerizes slowly.

Remember the fact that the NPMI monomers reduced at a lower electrical potential (−1.7 V) than 4-CPM (Table II); the reduced product is succinimide. The NPMI monomer does not electropolymerize at all without a comonomer such as styrene. This was found by a CV/FTIRS study.[19] It may be possible that having less reduction of NPMI in the electropolymerization of 4-CPM/NPMI by lowering NPMI concentration leads to an increase in the rate of polymer weight gain and the $\overline{M_n}$ (Table IX).

The electropolymerization temperature was

Table IX Kinetics Analysis of Electropolymerization of 4-CPM/NPMI

Test No.	Reaction Temperature (°C)	Monomer Conc.[a] (M/L) (4 cpm : npmi)	Current Density (mA/g)	Reaction Time (min) 10	20	30	60	R_p (%[c]/min)	$\overline{M_n}$ ($\times 10^{-4}$ g/mol)	$\overline{M_w}/\overline{M_n}$
1	28	0.5(80 : 20)	20	6.23	12.5	18.7	25.5	0.623	5.98	3.4
2	28	0.5(80 : 20)	30	7.92	15.9	23.9	30.6	0.792	5.35	3.2
3	28	0.5(80 : 20)	40	9.60	19.4	29.1	35.3	0.951	4.11	3.3
4	28	0.5(80 : 20)	30	7.65	15.5	23.2	31.3	0.765	5.06	3.0
5	28	0.6(80 : 20)	30	9.30	18.5	28.1	37.1	0.93	5.21	3.3
6	28	0.7(80 : 20)	30	11.5	22.9	34.3	43.8	1.15	5.56	3.2
7	28	0.5(70 : 30)	30	4.50	8.95	17.9	25.3	0.46	3.21	3.0
8	28	0.5(80 : 20)	30	8.20	15.5	24.5	32.6	0.82	5.11	3.3
9	28	0.5(90 : 10)	30	10.8	20.5	31.2	40.1	1.07	7.83	3.2
10	28	0.5(95 : 05)	30	9.95	19.8	30.5	38.8	0.99	7.72	3.0
11	28	0.5(90 : 10)	30	9.82	21.9	30.1	41.5	1.00	8.12	3.1
12	35	0.5(90 : 10)	30	13.5	27.4	40.3	51.5	1.39	7.69	3.0
13	45	0.5(90 : 10)	30	16.6	33.1	48.5	63.6	1.71	7.23	3.3

[a] H_2SO_4 conc.: 0.0125*M*.
[b] (%) g of polymer per g of graphite fiber.

raised from 28°C to 50°C for the 4-CPM/NPMI system. At 50°C reaction temperature, the polymer generated on the fiber surfaces fell almost completely to the bottom of the electrochemical cell. At lower temperature and a given monomer feed ratio, the polymer weight gain increased dramatically as the temperature was raised from 28°C to 45°C (Table IX). The increase in R_p as a result of increasing reaction temperature did not come from increasing the initiation rate as predicated from classical free-radical model equations, since the electropolymerization was run under constant current density (constant initiation rate). Therefore, the increased R_p was likely caused by increase of k_p (propagation rate constant) or to an increase in the diffusion coefficients of monomers and/or free radicals. Enhancement of the rate of electropolymerization by temperature increase was also reported by Samal and Nayak.[32] They studied the electropolymerization of acrylamide occurring by a combined radical and anionic mechanism in acetonitrile solvent.

The $\overline{M_n}$ value decreased slightly with increasing temperature, but the $\overline{M_n}$ values were still acceptably high (Table IX). Since the rate of polymer weight gain was increased dramatically with increasing temperature, this parameter will play a very important role for electropolymerization of other monomers that exhibit a low reaction rate at room temperature.

The usual treatment of classical free-radical copolymerization with thermal initiation cannot completely describe the kinetics of electropolymerization. For a thermally initiated polymerization, the degree of polymerization decreases rapidly with increasing temperature.[33] In contrast, for a pure photochemical polymerization, the degree of polymerization increases moderately with temperature.[34] Therefore, the temperature dependence of the degree of polymerization can be quite different depending on the nature of the initiation process.

Conclusions

Thick, random copolymers of 2- and 4-CPM/MMA, and 4-CPM/NPMI with high T_gs (200°C–300°C) have been electropolymerized onto the surfaces of AS4 graphite fibers. The copolymer composition can be controlled by the ratio of monomers in the solution, with T_gs following the behavior expected from random copolymers. The copolymer composition is consistent with free radical polymerization kinetics[35] in terms of the effects of monomer feed ratio, current density, and monomer concentration.

Interactions within the monomer pairs of 4-CPM/MMA, 2-CPM/MMA, and 4-CPM/NPMI have increased the electropolymerization rate. A high polymer weight gain (more than 60%) on graphite fibers in a short time was found for these monomer combinations. In contrast, the high polymer weight gain was not found for 4-CPM, 2-CPM, and NPMI monomers alone. The details of the nature of the interaction are unclear, but the interaction of comonomers was demonstrated by the cyclic voltammetry and the cyclic voltammetry/FTIRS studies.

The diffusion of active species can be improved by optimizing the DMAc/water solvent ratio to provide optimum swelling of the polymer coating on the graphite fibers. The DMAc/water ratio can be increased until copolymer dissolution begins. The DMAc/water ratio dependence of the diffusion behavior of reactive species was demonstrated by the electrochemical performance of polymer-coated electrodes. As the DMAc concentration is increased, an increase in the diffusion coefficient and the mass transfer of reactive species occurs.

The kinetics of the electropolymerization of 4-CPM/MMA and 4-CPM/NPMI were consistent with a free-radical mechanism. Evidence was provided by experiments following DPPH consumption as a function of time, by cyclic voltammetry/FTIRS, and by monomer-reactivity analysis. The electropolymerization rate increased with increasing current density, monomer concentration, and temperature. For a slight temperature increase (from 28°C to 45°C), electropolymerization rate and polymer weight gain increased dramatically for the 4-CPM/NPMI system. The $\overline{M_n}$ of 4-CPM/NPMI copolymer decreased only slightly with increasing temperature.

The authors wish to acknowledge the support of this research by the Connecticut Department of Higher Education.

REFERENCES

1. A. F. Yee, Polymers for Composites Conference, Solihull, West Midlands, U.K., Dec. 1987, Plastics and Rubber Institute, London, Paper 9.
2. D. M. Carlin, Society of Plastics Engineers, Transactions of ANTEC'89, p. 1447.
3. S. D. Mills, 21st International SAMPE Technical Conference September 25–28, 1989.
4. J. E. O'Connor, *SAMPE Quart.*, **18**(3), 32–38 (1987).
5. H. M. Colquhoun, P. D. Mackenzie, P. T. McGrail, and E. Nield, Polymers for Composites Conference,

Solihull, West Midlands, U.K., Dec. 1987, Plastics and Rubber Institute, London, Paper 6.
6. R. V. Subramanian and J. J. Jakubowski, *Polym. Eng. Sci.*, **18,** 590 (1978).
7. R. V. Subramanian, *Adv. Polym. Sci.*, **33,** 34 (1979).
8. J. Chang, J. Bell, and R. Joseph, *SAMPE Quan.*, **18,** 39–45 (1987).
9. J. P. Bell, J. Chang, H. W. Rhee, and R. Joseph, *Polym. Composites,* **8,** 46–52 (1987).
10. J. Iroh, J. P. Bell, and D. A. Scola, SPE/APC Conference on Advanced Polymer Composites for Structural Applications, Los Angeles, CA, Nov. 11–17, 1988.
11. J. Iroh, J. P. Bell, and D. A. Scola, *J. Appl. Polym. Sci.*, **41,** 735 (1990).
12. J. Iroh, J. P. Bell, and D. A. Scola, *J. Appl. Polym. Sci.*, to appear.
13. J. Iroh, J. P. Bell, and D. A. Scola, *J. Appl. Polym. Sci.*, **43,** 2237–2247 (1991).
14. J. Iroh, J. P. Bell, and D. A. Scola, to appear.
15. H. Li, A. Moshonov, and J. D. Muzzy, *Polym. Composites,* **12,** 191 (1991).
16. J. R. MacCallum and D. H. Mackerron, *Brit. Polym. J.*, **14,** 14 (1982).
17. K. Patel, T. Desai, and B. Suthar, *Makromol. Chem.*, **186,** 1151–1156 (1985).
18. C. K. Sauers, *J. Org. Chem.*, **34,** 2275 (1969).
19. J. L. Liang, Ph.D. thesis, University of Connecticut, 1991.
20. M. C. Pham, F. Adami, and J. E. Dubois, *J. Electrochem. Soc.*, **134,** 2166 (1987).
21. S. J. Porter, C. L. DeArmitt, R. Robinson, J. P. Kirby, and D. C. Bott, *High Perf. Polym.*, **1,** 85 (1989).
22. A. F. Shaaban and A. A. Khalil, *J. Appl. Polym. Sci.*, **37,** 2051–2058 (1989).
23. J. R. MacCullum and D. H. MacKerron, *Eur. Poly. J.*, **18,** 717 (1982).
24. T. Otsu, A. Matsumoto, T. Kubota, and S. Mori, *Polym. Bull.*, **23,** 51–56 (1990).
25. A. J. Bard and L. R. Faukner, *Electrochemical Methods,* John Wiley & Sons, New York, 1980, p. 218.
26. P. J. Peerce and A. J. Bard, *J. Electroanal. Chem. Interfacial Electrochem.*, **112,** 97–115 (1980).
27. L. Meites and Y. Israel, *J. Amer. Chem. Soc.*, **83,** 4903–4906 (1962).
28. M. Fineman and S. D. Ross, *J. Polym. Sci.*, **5,** 269 (1950).
29. J. N. Atherton and A. M. North, *Trans. Faraday Soc.*, **58,** 2049 (1962).
30. K. Ito, *Polym. Commun.*, **29,** 223 (1988).
31. K. Kojima, S. Iwabuchi, M. Kunagi, J. Kikuchi, and K. Iida, *Chiba Daigaku Kongakubu Kenkyuhoukoku,* **25,** 65 (1974).
32. S. K. Samal and B. Nayak, *J. Polym. Sci., Polym. Chem. Ed.*, **26,** 1035–1049 (1988).
33. A. Roche and C. C. Price in *Styrene: Its Polymers, Copolymers, and Derivatives,* R. H. Boundy, R. F. Boyer, and S. M. Stoesser, Eds., Van Nostrand Reinhold, New York, 1952, p. 216.
34. G. Odian, *Principles of Polymerization,* John Wiley & Sons, New York, 1981, p. 262.
35. J. P. Bell, J. Iroh, W. Kim, and D. A. Scola, Society of Plastics Engineers, Transactions of ANTEC'89, p. 565.

Received February 7, 1992
Accepted July 25, 1992